Metabolic Engineering 77 (2023) 231–241

Contents lists available at ScienceDirect

Metabolic Engineering

journal homepage: www.elsevier.com/locate/meteng

Silk fibroin production in *Escherichia coli* is limited by a positive feedback loop between metabolic burden and toxicity stress

Zhengyang Xiao [b,1], Alexander J. Connor [a,1], Alyssa M. Worland [b], Yinjie J. Tang [b,**], R. Helen Zha [a,***], Mattheos Koffas [a,*]

[a] Department of Chemical and Biological Engineering, Rensselaer Polytechnic Institute, Troy, NY, 12180, USA
[b] Department of Energy, Environmental and Chemical Engineering, Washington University in St. Louis, St. Louis, MO, 63130, USA

ARTICLE INFO

Keywords:
^{13}C-MFA
Acetate overflow
Entner–doudoroff pathway
Metabolic burden
Silk fibroin
Toxicity

ABSTRACT

To investigate the metabolic elasticity and production bottlenecks for recombinant silk proteins in *Escherichia coli*, we performed a comprehensive characterization of one elastin-like peptide strain (ELP) and two silk protein strains (A5 4mer, A5 16mer). Our approach included ^{13}C metabolic flux analysis, genome-scale modeling, transcription analysis, and ^{13}C-assisted media optimization experiments. Three engineered strains maintained their central flux network during growth, while measurable metabolic flux redistributions (such as the Entner–Doudoroff pathway) were detected. Under metabolic burdens, the reduced TCA fluxes forced the engineered strain to rely more on substrate-level phosphorylation for ATP production, which increased acetate overflow. Acetate (as low as 10 mM) in the media was highly toxic to silk-producing strains, which reduced 4mer production by 43% and 16mer by 84%, respectively. Due to the high toxicity of large-size silk proteins, 16mer's productivity was limited, particularly in the minimal medium. Therefore, metabolic burden, overflow acetate, and toxicity of silk proteins may form a vicious positive feedback loop that fractures the metabolic network. Three solutions could be applied: 1) addition of building block supplements (i.e., eight key amino acids: His, Ile, Phe, Pro, Tyr, Lys, Met, Glu) to reduce metabolic burden; 2) disengagement of growth and production; and 3) use of non-glucose based substrate to reduce acetate overflow. Other reported strategies were also discussed in light of decoupling this positive feedback loop.

1. Introduction

Silk proteins are of intense interest to researchers due to their unparalleled combination of chemical and physical properties, varied morphologies, and diverse applications. Dragline silk protein from orb-weaving spiders is of particular interest as it exhibits robust mechanical properties (Gosline et al., 1999; Hardy et al., 2008). Moreover, dragline silk fibroin (dragline spidroin) is a biodegradable polymer that can be processed into a diverse array of morphologies. As such, the applications of silk range from next-generation body armor to optofluidic devices and even coatings for food preservation (Altman et al., 2003; Holland et al., 2019; Marelli et al., 2016; Motta et al., 2002; Sarkar et al., 2019; Tsioris et al., 2010; Vepari and Kaplan, 2007). The beneficial properties of orb-weaving spider dragline spidroins arise from their highly conserved primary sequences. In nature, these proteins are approximately 250–350 kDa (Gatesy et al., 2001). Approximately 90% of a dragline silk protein's primary sequence can be classified as a repetitive diblock copolymer comprised of a hydrophilic segment with high glycine, proline, and glutamine content alternating with a hydrophobic segment with high alanine content. When fibers are created from dragline spidroins, the polyalanine regions form beta-sheet-rich nanocrystals and the glycine-rich regions form an amorphous matrix. The interplay between these crystalline and amorphous regions imparts spider silk with a combination of high tensile strength and extensibility (Sarkar et al., 2019; Tokareva et al., 2014).

Unlike silkworm-derived materials, spiders cannot be farmed or harvested from nature on a large scale (Tokareva et al., 2013). The recombinant production of spider silk proteins is the most promising route

* Corresponding author.
** Corresponding author.
*** Corresponding author.
E-mail addresses: yinjie.tang@wustl.edu (Y.J. Tang), zhar@rpi.edu (R.H. Zha), koffam@rpi.edu (M. Koffas).
[1] These authors contributed equally to this work.

https://doi.org/10.1016/j.ymben.2023.03.011
Received 11 February 2023; Received in revised form 11 March 2023; Accepted 25 March 2023
Available online 5 April 2023

toward the production of customized spidroin sequences for targeted applications (Schmuck et al., 2021; Whittall et al., 2021; Yang et al., 2016). Due to difficulties in obtaining the cDNA of natural spidroins, researchers typically produce recombinant spidroins by creating synthetic genes that mimic a consensus sequence of natural spidroins. Recombinant silk has been produced in a variety of hosts, including bacteria (Bowen et al., 2018), yeast (Jansson et al., 2016), mammalian cells (Lazaris et al., 2002), transgenic plants (Scheller et al., 2004), and transgenic animals (Wen et al., 2010). Notwithstanding, the field of recombinant silk production suffers from several fundamental issues, chiefly a high cost of production that stems from low titers (Schmuck et al., 2021; Teulé et al., 2009; Whittall et al., 2021; Yang et al., 2016).

In recent work, a panel of *E. coli* strains was used to express four different *de novo* designed dragline spidroins (Connor et al., 2023). These polymeric silk constructs had similar amino acid sequences to natural dragline spidroin, including two small constructs (the ~16 kDa A5 4mer and A10 4mer) and two larger constructs (the ~50 kDa A5 16mer and A10 16mer). A novel strain of *E. coli,* SoluBL21-pLysS, was created and found to produce the recombinant spidroins at levels 4–33 times higher than standard BL21, but this novel strain offered no benefit over BL21 for the production of an elastin-like peptide (ELP) with similar amino acid composition but less conformational disorder as the spidroins. It was found that there was toxicity during the expression of the recombinant spidroins (i.e., A5 4mer and A5 16mer), but not the ELP.

The overproduction of recombinant protein poses metabolic burdens on the cells (Kaleta et al., 2013), which requires the reorganization of the intrinsic metabolic flux network. Metabolic burden is defined as the portion of the cell's resources used to maintain growth and product synthesis (Glick, 1995). Moreover, stressed conditions (such as toxic products) may aggravate metabolic burdens by increasing maintenance expenditures. Although the engineered microbes are able to function normally under certain degrees of metabolic burdens, the cumulative burdens may fracture the flux network(Wu et al., 2016). Therefore, the metabolic flux rigidity determines cell bioproduction capability (Fischer and Sauer, 2005; Stephanopoulos and Vallino, 1991). Labeled ^{13}C glucose was used to resolve central metabolism fluxes in engineered *E. coli* strains that express a recombinant protein (Kayser et al., 2005, 2005z; Özkan et al., 2005). Metabolic flux analysis (MFA) can quantify metabolic burden (Heyland et al., 2011; Wu et al., 2016), confirm genetic engineering outcomes (Weber et al., 2002; Yang et al., 1999), and identify pathways related to high titer (Young, 2014). However, little has been known about *E.coli* metabolic elasticity for silk protein synthesis.

There were some studies regarding the challenges of obtaining high recombinant protein titer, including metabolic burdens (i.e., overuse of cellular resources), genetic heterogeneity (Rugbjerg and Sommer, 2019), tRNA shortages (Bowen et al., 2018), and stressed growth conditions (Collins et al., 2013). In general, nutrient supplements (amino acids) can alleviate stresses, but amino acids do not have equal contributions to biomass synthesis (Kumar et al., 2020). In a previous report, ^{13}C tracer identified 4 key amino acids supplement that enhanced *Dehalococcoides ethenogenes* growth at a level similar to supplementing all 20 amino acids (Zhuang et al., 2011). To have a holistic understanding of bottlenecks, product toxicity, and metabolic network rigidity during recombinant protein expression, this study employed ^{13}C-MFA, genome-scale model simulations, qRT-PCR, and ^{13}C-assisted medium optimizations to analyze and compare three engineered strains: a small spidroin (A5 4mer), a large spidroin (A5 16mer), and an elastin-like peptide (ELP).

2. Materials and methods

2.1. Bacterial cultivation

All experiments were carried out using *the E. coli* strain SoluBL21-pLysS (Connor et al., 2023), which was developed in prior work by our group. The pET19b vector (Addgene, Watertown, MA) was used to express the A5 4mer, A5 16mer, and ELP constructs. The sequences, construction, and transformation of all three recombinant genes were identical to previously described methods (Connor et al., 2023). For protein expressions, overnight cultures were inoculated with a single plated colony and grown at 37 °C in 5 mL LB media and placed in 15 mL conical tubes at an angle of ~55° with 225 rpm shaking. The media used for overnight cultures was identical to that used for expression cultures (i.e., for expressions in LB media, cells were grown overnight in LB media). Two milliliters of the overnight cultures were used to inoculate 50 mL expression cultures placed in 250 mL Erlenmeyer flasks with 225 rpm shaking. Recombinant protein production was induced with 1 mM isopropyl-β-D-thiogalactoside (IPTG; Sigma Aldrich, St. Louis, MO) when the cultures reached an OD600 of 0.6–0.8. All culture media and agar plates contained 25 μg/L of chloramphenicol and 100 μg/L of ampicillin. In rich media cultivation, standard LB media was used (10 g/L tryptone, 5 g/L yeast extract, and 10 g/L NaCl). In minimal media cultivation, M9 minimal media salts were used for media preparation (Sigma Aldrich, St. Louis, MO). For titer calculations, the A5 4mer, A5 16mer, and ELP proteins were purified using a heat-treatment method, and the titer was quantified using methods identical to those previously described (Connor et al., 2023). For ^{13}C labeling experiments, the A5 4mer, A5 16mer, and ELP proteins were purified using nickel chromatography as previously described (Connor et al., 2023). The SDS-PAGE image is shown in Fig. S3.

2.2. Glucose consumption and acetate overflow measurements

Each time, 1 mL of the culture was taken out and centrifuged under 20000 g and 2 °C for 10 min. The supernatant was drawn to a new tube and stored at −20 °C until measurements. Glucose and acetate concentrations were measured using a UV absorbance enzyme kit (manufactured by R-Biopharm AG, Germany). A UV–vis spectrometer (Agilent Cary-60) was used to measure the absorbance at 340 nm.

2.3. ^{13}C labeling experiment

^{13}C labeled glucose was purchased from Cambridge isotope laboratories. In MFA experiments, 4 g/L 1,2–^{13}C glucose was used. After LB seed culture, the strains were cultured into a second seed culture with ^{13}C labeled glucose to minimize carry-over. Then the second seed culture was used to inoculate the ^{13}C experiment culture. The inoculation ratio was 0.5% v/v. At OD600 of 0.3, 1 mM of IPTG was added to express the recombinant protein gene. The proteinogenic amino acids sampling procedure followed our published protocol (Hollinshead et al., 2019; You et al., 2012). The purified silk proteins were hydrolyzed similarly. The TBDMS derivatized amino acids were analyzed by a GC-MS system (Agilent gas chromatography 7820A with HP-5m column and 5977E MSD). The GC condition followed the method in a previous study (Au - You et al., 2012). The free metabolite sampling procedure followed our published protocol and was analyzed by a ThermoFisher TSQ Altis LC-MS system (Czajka et al., 2020). The mass isotopomer distribution (MID) data were corrected for natural isotope abundance and processed by an open-source software WUflux (He et al., 2016), which calculates metabolic flux distributions in central metabolism.

In the amino acid uptake experiment, the growth media contained 4 g/L U–^{13}C glucose and 0.05 g/L of each of the 20 amino acids. Strains were cultured into ^{13}C labeled media before inoculating into the expression culture to minimize carry-over. At OD600 of 0.6–0.7, 1 mM of IPTG was added to express the recombinant protein gene. After induction, an additional 0.25 g/L each of alanine, glycine, glutamine, and proline was added to the culture to support recombinant protein production. Four hours after IPTG induction, 10 mL of culture was harvested for proteinogenic amino acids MID analysis, and 50 mL was sampled for subsequent recombinant protein purification.

2.4. Genome-scale model cofactor balance

We used the COBRApy package for the flux balance analysis (Ebrahim et al., 2013). A BiGG *E. coli* model iJO1366 was used (Hädicke and Klamt, 2017). The recombinant protein production reaction (ELP/A5 4mer/A5 16mer) was added to the model as a one-step, lumped reaction with corresponding amino acids stoichiometry and 4.3 mol ATP/mol amino acids condensation cofactor costs. The protein production reaction fluxes were set to the experimental titers, and the model's objective was set to the biomass equation. When using ^{13}C MFA results to constrain the model, key reactions in the central metabolism were constrained to the MFA flux calculation, with standard deviation as upper and lower bounds. The reactions constrained were: *PGI, PFK, CS, ACONTb, SUCOAS, SUCDi, FUM, MDH, PPC, ICL, MALS, PGL, GND, EDA,* and *ACtex*. All constraints except the silk protein production were removed when simulating the "optimal" flux distribution. The summary function displayed the cofactor production/consumption reactions in COBRApy.

2.5. qRT-PCR

For qRT-PCR, cell cultures were cultivated in M9 minimal media supplemented with 4 g/L glucose using the same procedures as described above for protein expressions. Two sets of cultures were analyzed, with one harvested directly before induction at an OD600 of 0.6–0.8 and the other harvested 4 h after induction with 1 mM IPTG. RNA was extracted from the cells using the RNeasy Mini Kit (Qiagen, Germantown, MD) according to the manufacturer's protocol. The qRT-PCR was performed using the iTaq Universal SYBR Green One-Step Kit (Bio-Rad, Hercules, CA) and the CFX96 Real-Time PCR system (Bio-Rad, Hercules, CA) according to the manufacturer's protocol. All RT-PCR reactions were run in triplicate using 10 μl reactions in a 96-well PCR plate. Data were analyzed using the CFX Manager software (Bio-Rad, Hercules, CA). All primers used for the qRT-PCR are listed in Supplementary Table 1.

3. Results and discussion

3.1. Growth characteristics and production titers of the engineered E. coli strains in M9 minimal media

In many cases, recombinant protein production uses rich media. In contrast, minimal media that use well-defined sugar feedstocks, such as glucose, are of interest due to their known compositions and better production control (Cardoso et al., 2020). Although all three protein constructs were successfully produced in the minimal media, the titer and cell growth during expression decreased by 5-8x across all constructs when transitioning from the LB to the minimal media. Table 1 is a conceptual summary of the three engineered strains used in this study. We selected ELP as a low-toxicity recombinant protein with similar amino acid composition as silk fibroin. As tabulated in Table S1, the A5 silk proteins contain a 35 amino acid segment that is rich in GPGQQ motifs and contains a run of five tandem alanines. This segment is repeated sequentially either 4 or 16 times to form the A5 4mer or A5 16mer. The elastin-like peptide is comprised primarily of VPGAG repeats, and when compared to the A5 4mer, it contains a similar glycine, proline, and alanine content as well as nearly identical molecular weight. In agreement with previous expression in LB media, expression of the A5 4mer or A5 16mer appears more toxic to the host than the expression of the ELP in the minimal media, as shown by their considerably lower final OD_{600} (Connor et al., 2023). We consider silk fibroin has a higher metabolic burden because they mainly contain glutamine, a high-energy amino acid. The A5 16mer has a larger size and longer mRNA. It is possible that A5 16mer expression leads to increased competition among the available ribosomes and reduces the cellular capacity for housekeeping protein synthesis (Hoffmann and Rinas, 2004). Therefore, we consider A5 16mer as the most toxic construct in this study. Control (uninduced strain), ELP, A5 4mer, and A5 16mer strains were cultivated in M9 + 4 g/L glucose and LB under 37 °C and aerobic conditions. Their final production titers are ELP 28.1 mg/L, A5 4mer 37.4 mg/L, and A5 16mer 6.0 mg/L. The three strains had acetic acid overflow when expressing the recombinant protein in M9 + 4 g/L glucose. We normalized the acetate overflow per 100 mmol glucose consumption. Compared to the uninduced control 20.3 mmol/h, engineered strains showed higher acetate overflow flux during protein expression: ELP 29.7 mmol, A5 4mer 35.8 mmol, and A5 16mer 30.6 mmol. When *E. coli* cells are under pressure (product stresses and metabolic burdens), their oxidative phosphorylation (NADH - > ATP) at the outer membrane will be less efficient for ATP generation (P/O ratio <2). Therefore, acetate overflow is an alternative way to meet the ATP demand (Shuler and Kargi, 2002). The observed highest acetate overflow is consistent with the highest recombinant protein production in A5 4mer. The glucose consumption and acetate overflow were measured and later used to constrain the MFA model.

Table 1
A conceptual summary of the three engineered strains.

Strain	ELP	A5 4mer	A5 16mer
Product description	Elastin-like peptide	Small silk fibroin	Large silk fibroin
Number of residues	184	170	590
Major amino acids (mol %)	Ala (13%), Gly (36%), Pro (16%), Val (16%)	Ala (12%), Gly (33%), Pro (15%), Gln (21%)	Ala (14%), Gly (36%), Pro (16%), Gln (24%)
Metabolic burden	Low	Medium	Medium
Product toxicity	Low	Medium	High

3.2. Central metabolic fluxes and metabolic elasticity

To elucidate the distribution of central metabolic pathway fluxes, we carried out ^{13}C tracer experiments on 4 strains: control, ELP, A5 4mer, and A5 16mer. One time point was sampled during the mid-exponential phase. The labeling patterns (or mass isotopomer distributions, MID) are tabulated in Supplementary file 2. Similar to previous studies (Heyland et al., 2011; You et al., 2015), we used purified proteins as reporters and compared their MID with that of biomass amino acids (Fig. 1). For all three strains, the MID in purified protein and biomass follows the y = x line, with high R^2 values, so we confirmed a pseudo steady-state, and the uninduced growth phase had little effect on the final flux calculation. We also measured fast-turnover free metabolites using LC-MS and included G6P, F6P, GAP, PEP, and succinate in the flux calculations. The computationally simulated MID and measured MID followed the y = x line with high R^2 values and acceptable sum of squared residuals (SSR) (Supplementary file 2), demonstrating that the cells reached an approximate metabolic steady-state after IPTG induction and making our steady-state MFA reliable. We noticed that in A5 4mer and 16mer constructs, the correlation coefficient R^2 slightly decreased (Fig. 1), implying that the metabolic networks of silk-producing strains had small perturbations after induction and deviated slightly from the metabolic steady-state. The A5 16mer had the highest change due to metabolic burden and product toxicity.

We generated the flux map in Fig. 2 using WUFlux, an open-source MATLAB software developed by our group (He et al., 2016). Overall, three engineered strains maintained normal central metabolism during induction. In terms of absolute flux values, the three engineered strains were similar to each other. Previous work showed that the A5 16mer shows a higher level of toxicity. This may explain the differences in production levels despite their similar metabolic fluxes (Connor et al., 2023). We summarized four measurable flux redistributions: (1) The most significant changes in the central metabolism were the TCA cycle

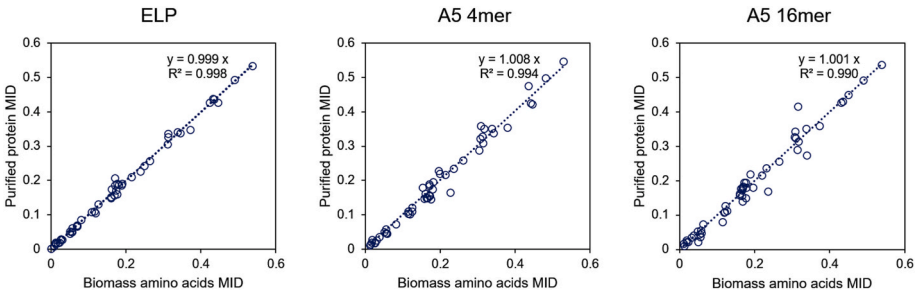

Fig. 1. Purified protein MID versus biomass amino acids MID in strains ELP, A5 4mer, and A5 16mer.

fluxes, likely caused by an increase in the acetate overflow and a decrease in the cytosolic acetyl-CoA pool. The reduced TCA cycle fluxes limited the availability of ATP and amino acid precursors for recombinant protein synthesis. (2) The glyoxylate shunt became more active in three engineered strains, indicating a response to oxidative stress (Rui et al., 2010). (3) Acetate overflow metabolism increased in all three engineered strains, suggesting higher ATP demand (Hoffmann and Rinas, 2004). (4) The Entner–Doudoroff (ED) pathway was upregulated in all three engineered strains. As the three recombinant proteins are rich in alanine and glycine, the ED pathway was activated to compensate for the consumption of the precursors of alanine and glycine, 3PG, and pyruvate. ED pathway activation in *E. coli* is uncommon as it produces less ATP than the EMP pathway. However, the ED pathway requires fewer enzymatic steps than the Embden-Meyerhof-Parnas (EMP) pathway, providing a short route for downstream amino acid precursors supply (Flamholz et al., 2013). This scaffold strain (control) had a higher basal level of ED pathway than *E. coli* K12 DH1 strain (He et al., 2014). The EMP pathway was still the dominant glucose catabolic pathway. The ED pathway was reported to be a rigid node in the central metabolism, with small changes in response to genetic perturbations (He et al., 2014), and it was suggested that rigid nodes are good targets for metabolic engineering (Hollinshead et al., 2016; Stephanopoulos and Vallino, 1991).

3.3. Genome-scale model (GSM) cofactor balance

Using metabolic fluxes determined by ^{13}C MFA as constraints, we loaded a COBRA model iJO1366 to simulate a genome-scale flux distribution and cofactor production/consumption. Two data sets were generated with biomass equation as their objectives and the recombinant protein production reactions were set to the experimental titers. In the first set, the model calculated genome-wide reaction data with key reactions in the central metabolism constrained by ^{13}C MFA experiment results. In the second set, the model simulated "optimal" flux distributions. Note that the genome-scale model doesn't consider the product toxicity for the A5 16mer, so we excluded this strain from modeling and discussion. Tables 2 and 3 summarizes the simulation results, with the reactions of interest marked with an asterisk. For the modeling constrained by ^{13}C MFA results, we summarized our findings below. (1) In two engineered strains, compared to the control, the total ATP produced was 10% lower in ELP and 9% lower in A5 4mer. (2) As TCA cycle fluxes decreased in the engineered strains, isocitrate dehydrogenase (ICDH) supplied less NADPH compared to control, −26% in ELP and −32% in A5 4mer. (3) The C1 metabolism Methylenetetrahydrofolate dehydrogenase (MTHFD) was upregulated to compensate for the NADPH shortage, 3.4-fold in ELP and 4-fold in A5 4mer. (4) The recombinant protein is rich in proline and glutamine, so the glutamate synthesis reaction GLUDy consumed more NADPH in the engineered strain, 5% more in ELP and A5 4mer. (5) The reduction from glutamate to glutamine (GLNS, glutamine synthetase) consumed more ATP in the engineered strain, with increases of 185% in ELP and 208% in A5 4mer.

The "optimal" flux distribution in a GSM refers to a set of flux distributions that maximizes the objective function. However, other alternative flux distributions also exist (O'Brien et al., 2015). During actual cultivation processes, bacteria usually have suboptimal flux distributions (Fischer and Sauer, 2005; San Román et al., 2014), as indicated by the lower ATP consumption for biomass formation across all three strains. It seems that all three cofactors are limiting in the engineered strain. By comparing GSM "optimal" and ^{13}C MFA measured fluxes, we can understand the bottlenecks in cofactors (Wu et al., 2016). (1) In "optimal" simulations, ELP and A5 4mer produced a larger percentage of ATP through oxidative phosphorylation. (2) Under "optimal" conditions, TCA cycle fluxes were upregulated. More NADPH and NADH would have been produced by isocitrate dehydrogenase (ICDH) and malate dehydrogenase (MDH), respectively. (3) Glutamate production would have consumed more NADPH under optimal conditions, but in actual situations, the reaction glutamine synthetase (GLUDy) was limited by NADPH shortage.

3.4. Confirmation of Entner Doudoroff pathway

The Entner Doudoroff (ED) pathway has fewer enzymatic steps and faster kinetics than either the Embden–Meyerhof–Parnas (EMP) pathway or the oxidative pentose phosphate (OPP) pathway (Flamholz et al., 2013). However, this pathway produces less ATP than the EMP pathway. While the ED pathway is mainly activated by gluconate metabolism, *E.* coli can shuttle glucose through this pathway via glucose-6-phosphate dehydrogenase (Hollinshead et al., 2016). The use of this pathway may increase the precursors (Glyceraldehyde 3-phosphate and pyruvate) available for recombinant silk and ELP synthesis. The relative activity of the ED pathway during A5 4mer, A5 16mer, and ELP production in M9 minimal media with 4 g/L glucose was quantified using qRT-PCR on the *edd* (6-phosphogluconate dehydratase) and *eda* (2-dehydro-3-deoxy-phosphogluconate aldolase) genes. Fig. 3 shows the fold difference in *edd* and *eda* gene expression after induction. Values are normalized by the housekeeping gene *gapdh*. This data shows that there is a 3.28- and 2.01-fold increase in *edd* gene expression during A5 4mer and A5 16mer production, respectively, when compared to uninduced cultures. Likewise, production of the A5 4mer and A5 16mer causes a 1.6-fold increase in the expression of the *eda* gene. However, ELP expression seems to negligibly change *edd* expression, with a 1.14-fold increase. Similarly, ELP production has no effect on *eda* expression as it shows only a 0.99-fold decrease. This indicates an increased need for central metabolism precursors and metabolic burden during silk production, but little effect with ELP. It seems that ED pathway activation is not related to protein size, but rather to the level of metabolic burden. A5 4mer and ELP were similar in size, but they showed a difference in ED pathway expression. A5 16mer has high product toxicity and low production titer, so its real-time burden is lower than A5 4mer, hence the lower ED pathway expression.

With qRT-PCR data showing upregulation of the ED pathway for silk production, we investigated whether targeted upregulation of the ED pathway may increase silk titers. The expressions of the A5 4mer, A5 16mer, and ELP were carried out in M9 minimal media supplemented

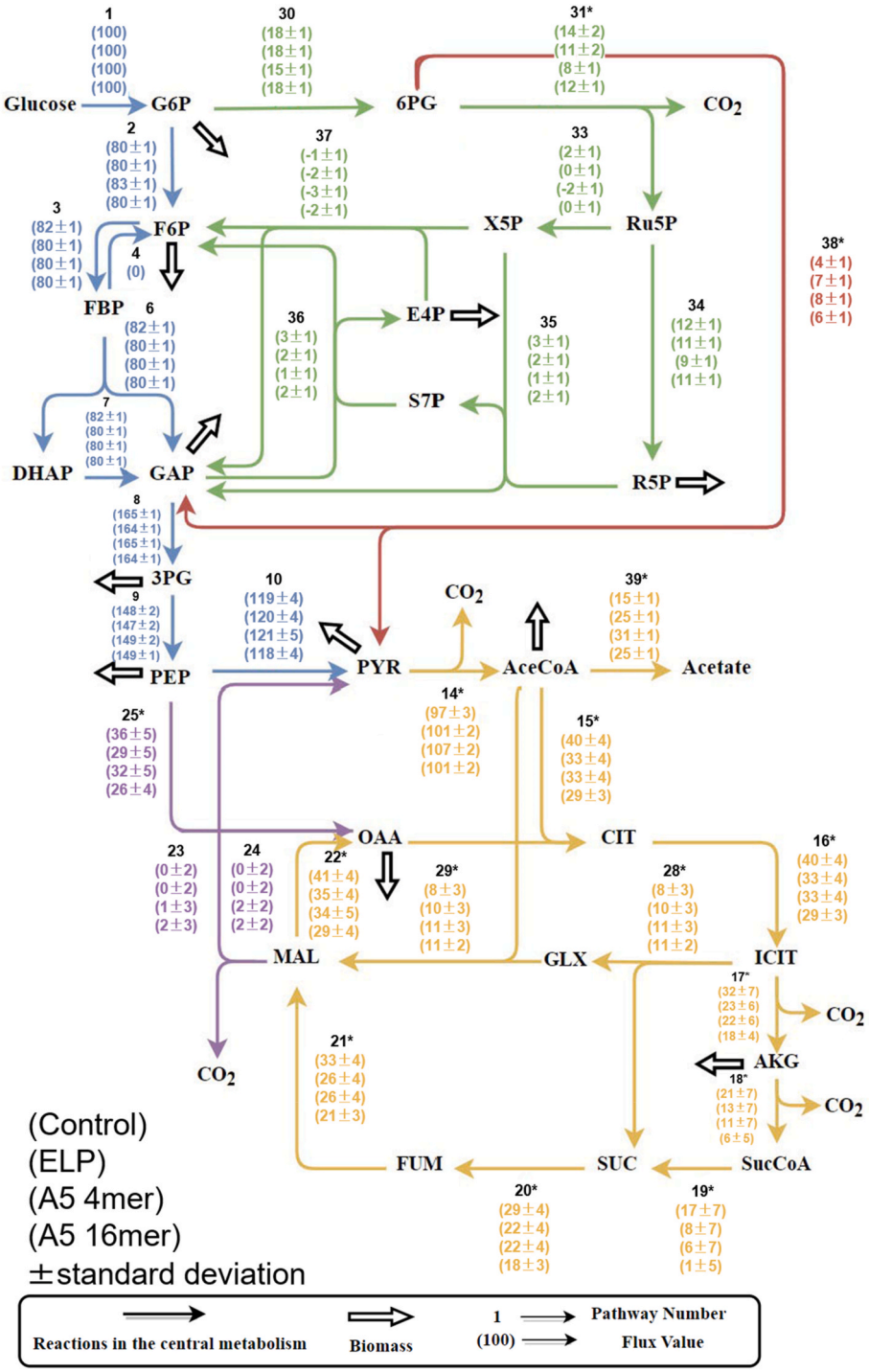

Fig. 2. Metabolic flux distributions in the central metabolic pathways of control, ELP, A5 4mer, and A5 16mer strains. The plus-minus sign shows the standard deviations. 95% confidence intervals are tabulated in the supplementary information. *Reactions of interest were marked with an asterisk.
Note: the standard deviation is calculated as one-fourth of the confidence interval during flux calculation.

with 4 g/L of sodium gluconate. Results showed that the titers of the three constructs did not change in a significant way when gluconate instead of glucose was supplied (Table 5). The titer of the A5 4mer increased slightly from 37 to 43 mg/L, while the titer of the A5 16mer decreased from 6 to 4.1 mg/L. The ELP titer also slightly decreased from 28.1 to 20.2 mg/L. It is possible that the decrease in ATP availability when using the ED pathway offsets any benefits garnered from the increase in the availability of metabolic precursors and reduced enzymatic costs [34]. To investigate this further, recombinant protein production was carried out in rich LB media in conjunction with the addition of 20 g/L gluconate or glucose. In this context, the cells have little restriction on energy supply due to the high nutrient density of LB media in combination with a surplus of sugar. The presence of gluconate or glucose will simultaneously upregulate the ED pathway [34,39]. Table 5 shows that the addition of gluconate to LB media had a positive effect on production levels when compared to M9 minimal media with either 4 g/L gluconate or glucose. Gluconate or glucose supplementation to LB media increased the titer of the A5 4mer to 61 mg/L. Gluconate supplementation increased the A5 16mer to 10 mg/L, while glucose supplementation increased the titer further to 12 mg/L. For the ELP,

Table 2
Cofactor production in GSM flux balance analysis simulations.

		Control		ELP		A5 4mer	
		With constraints from ^{13}C MFA	GSM "optimal"	With constraints from ^{13}C MFA	GSM "optimal"	With constraints from ^{13}C MFA	GSM "optimal"
ATP	Total	600	769	541	769	547	769
	Oxidative phosphorylation	387	542	346	544	339	546
	Others	213	227	195	225	208	223
NADPH	Total	114	106	99	148	97	149
	ICDH[a]	31	34	23	43	21	42
	G6PDH	17	21	19	42	16	41
	GND	14	17	12	42	9	41
	MTHFD[a]	5	6	17	21	20	24
	Others	47	0	28	0	31	0
NADH	Total	346	349	308	350	315	351
	GAPD	159	162	151	155	153	153
	PDH	77	78	99	70	102	69
	MDH[a]	47	46	31	55	30	57
	Others	63	63	27	70	30	72

Note: The unit is mmol. The fluxes were normalized to 100 mmol glucose consumption rate. A5 16mer was excluded from the discussion due to product toxicity.
Abbreviations: ICDH, isocitrate dehydrogenase; G6PDH, glucose-6-phosphate dehydrogenase; GND, phosphogluconate dehydrogenase; MTHFD, methylenetetrahydrofolate dehydrogenase; GAPD, glyceraldehyde-3-phosphate dehydrogenase; PDH, pyruvate dehydrogenase; MDH, malate dehydrogenase.
[a] Reaction of interest.

Table 3
Cofactor consumption in GSM flux balance analysis simulations.

		Control		ELP		A5 4mer	
		With constraints from ^{13}C MFA	GSM "optimal"	With constraints from ^{13}C MFA	GSM "optimal"	With constraints from ^{13}C MFA	GSM "optimal"
ATP	Total	600	769	541	769	547	769
	Biomass formation	298	538	257	469	227	453
	PFK	80	70	79	74	79	64
	GLNS[a]	13	18	24	28	27	31
	Others	209	143	181	198	214	221
NADPH	Total	114	106	99	148	97	149
	GLUDy[a]	62	60	65	98	65	100
	Others	52	46	34	50	32	49
NADH	Total	346	349	308	350	315	351
	Oxidative phosphorylation	303	302	204	310	205	312
	Others	43	47	104	40	110	39

Note: The unit is mmol. The fluxes were normalized to 100 mmol glucose consumption rate. A5 16mer was excluded from the discussion due to product toxicity.
Abbreviations: PFK, phosphofructokinase; GLNS, glutamine synthetase; GLUDy, glutamate dehydrogenase (NADP).
[a] Reaction of interest.

gluconate supplementation increased the titer to 41 mg/L, while adding glucose to the LB did not have a significant effect. These results show that activation of the ED pathway is favorable for the production of these proteins. However, this may only be the case when the media is rich enough to confer a surplus of ATP within the metabolism.

3.5. Uneven external amino acids supplement and uptake preference

The twenty amino acids are not equally important for cells, because of their different metabolic costs for synthesis in vivo (Kaleta et al., 2013). In theory, after ^{13}C labeling experiment reveals the rate-limiting amino acids, we can supplement the media accordingly to increase the biomass growth and production titer. We grew engineered strains with fully labeled U–^{13}C glucose and each of 20 unlabeled amino acids. Conceptually, a high ^{13}C fraction in a sampled proteinogenic amino acid indicates that the strain synthesizes that amino acid from glucose. On the contrary, if the sampled amino acid has a low ^{13}C labeled fraction, it means that the strain uptakes that amino acid from the media. The fraction of ^{13}C in each amino acid in the biomass is summarized in Fig. 4. It is worth noting that in our TBDMS derivatization method, glutamine and asparagine were oxidized to glutamate and aspartic acid, respectively, so the labeling fractions of these amino acids were lumped together. Cysteine and tryptophan cannot be analyzed by this TBDMS method (Hollinshead et al., 2019). We observed three amino acid groups (Table 4): 1. Some amino acids (Ala, Ser, Asp) had consistently high labeling fractions. 2. Some amino acids (Gly, Pro, His) had consistently low labeling fractions. 3. Most amino acids (Val, Leu, Ile, Met, Thr, Phe, Glu, Lys, Tyr) had a decreased labeling fraction in the engineered strain compared to the control strain. The engineered strain used these amino acids more than the control strain. The result from this experiment was used to guide the later media optimization in this study.

3.6. Media optimization to improve production titer

As mentioned previously, ^{13}C labeled experiments showed disparities in which amino acids were preferentially taken from the media. We ranked the labeling fraction in each amino acid from low to high (Supplementary Fig. S1). With a background of M9 minimal media and 4 g/L glucose, seven amino acids with the lowest labeling fraction were added (0.3 g/L each): histidine, isoleucine, phenylalanine, proline,

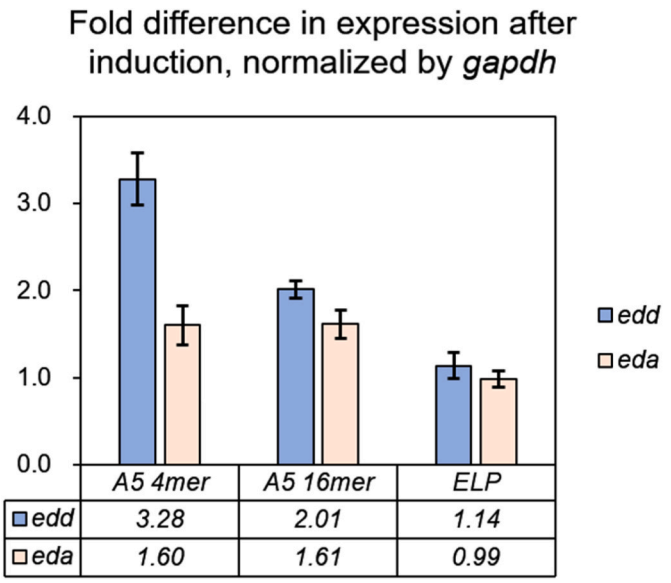

Fig. 3. qRT-PCR on *edd* and *eda* genes, normalized over *gapdh* activity (placeholder gene). Error bars represent standard deviations from the mean of two biological replicates.

tyrosine, lysine, and methionine. Supplementation of the amino acids to the media resulted in substantial increases in titer. The titer of the A5 4mer increased from 37 to 74 mg/L, the A5 16mer increased from 6 to 15 mg/L, and the ELP from 28 to 60 mg/L (Fig. 5). A5 16mer was dominated by the toxicity effect so its absolute increase in titer was small. For recombinant silk protein, this is the first documentation of increasing titers through the supplementation of select amino acids in which 6 out of the 7 amino acids are not major constituents of the recombinant protein, suggesting that sufficient host biomass is the prerequisite of recombinant protein synthesis. However, based on current data, it is not clear which individual amino acid or combination of amino acids had the greatest effect on the production titer.

In addition to ^{13}C labeling experiment, genome-scale modeling suggested that the glutamate production in the engineered strains consumed considerably more NADPH than the control. From here, 0.3 g/L of glutamate was supplemented to the cultures in addition to the seven amino acids. The addition of glutamate to the culture media further increased the titers of the A5 4mer and ELP but did not affect the A5 16mer production (Fig. 5). The increase in titer was most pronounced for the ELP protein. Adding 0.3 g/L glutamate yielded the same absolute increase in titer as adding a total of 2.1 g/L other seven amino acids.

To investigate the effect of glucose supplementation, we used the same amino acid supplementation with a higher glucose concentration (20 g/L). In theory, the surplus of glucose would facilitate greater ATP availability and increased titers. However, additional glucose decreased silk production, lowering the A5 4mer from 73 to 60 mg/L and the A5 16mer from 15 to 12 mg/L. In contrast, ELP production increased slightly, from 60 to 78 mg/L (Table 5, Fig. 6). Supplementing LB with 20 g/L of either gluconate or glucose lowered the titers of the constructs to approximately 1/8–1/3 of those obtained in normal LB media (Table 5). The large concentration of glucose or gluconate in the culture media hurts the recombinant protein production due to toxic acetic acid accumulation in the media (Eiteman and Altman, 2006; Suarez and Kilikian, 2000). The OD600 of each media alteration experiment is summarized in Table 6.

Our data shows that the limiting factor for ELP production was more heavily weighted towards central metabolism bottlenecks (ATP and NADPH), which can be alleviated by adding select amino acids. For the A5 4mer, the limiting factors are a combination of metabolic bottlenecks and product toxicity. The addition of exogenous amino acids promoted higher titers, but the response to glutamate was not as profound as the ELP. Limiting factors for A5 16mer, a large spidroin protein, were heavily weighted towards product toxicity and not metabolic stress, as the media optimization showed a limited effect. Across all constructs, utilization of sugar by the strain, specifically glucose and gluconate, was unfavorable for production levels when compared to LB media leading to the hypothesis that acetate overflow is harmful to the production of repetitive, structural proteins that are rich in alanine, glycine, and proline.

3.7. Acetate toxicity stress

The metabolism of glucose or gluconate leads to the production of acetate (Eiteman and Altman, 2006; Suarez and Kilikian, 2000), lowering intracellular pH and inducing acid stress (Luli and Strohl, 1990). Acetate stress is a factor behind inefficient recombinant protein production (Jensen and Carlsen, 1990), and this effect may be more pronounced for the production of the silk constructs due to their toxicity and amino acid composition (Connor et al., 2023). Transcriptomic data showed that acetate overflow inhibits the TCA cycle at the transcriptional level (Millard et al., 2021). Since the A5 4mer and A5 16mer silk proteins contain 21–24 mol% glutamine and 15–16 mol% proline (both

Table 4
Summarization of amino acids labeling.

Group	Characteristics	Amino acids
1	Consistently high fraction labeled	Ala, Ser, Asp
2	Consistently low fraction labeled	Gly, Pro, His
3	Lower fraction labeled in the engineered strain	Val, Leu, Ile, Met, Thr, Phe, Glu, Lys, Tyr

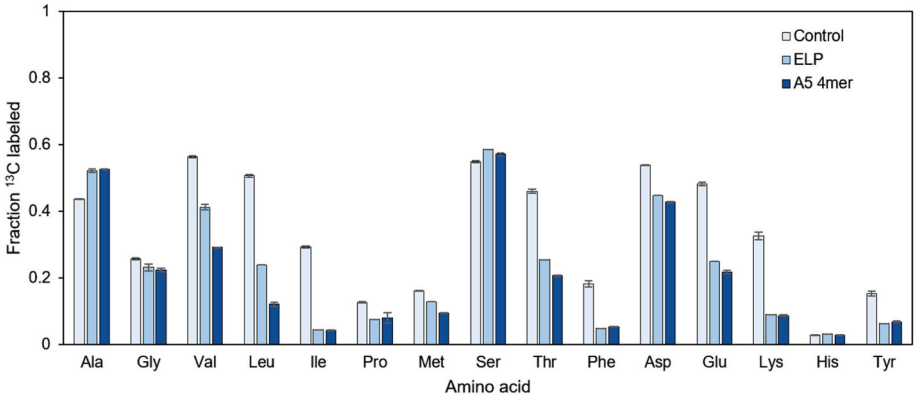

Fig. 4. Fraction of ^{13}C labeling in each amino acid in control, ELP, and A5 4mer strains. n = 2, ±standard deviation.

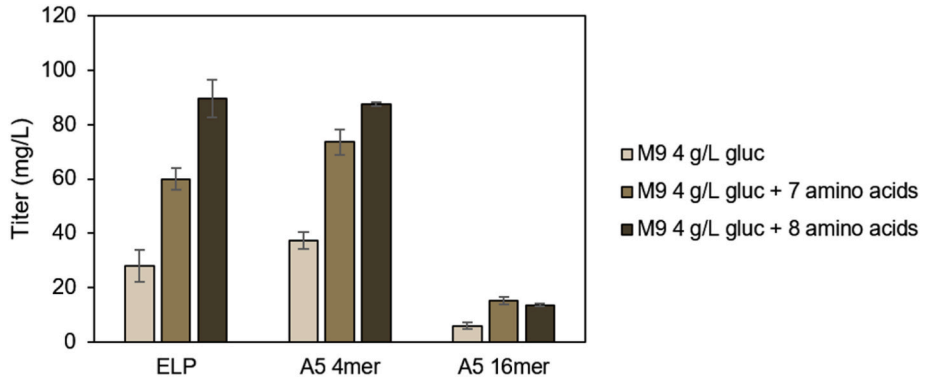

Fig. 5. Silk protein titers with amino acid supplementation. Note: The 7 amino acids are 0.3 g/L of each histidine, isoleucine, phenylalanine, proline, tyrosine, lysine, and methionine. The 8 amino acids are 7 amino acids plus 0.3 g/L glutamate. n = 3, ±standard deviation.

Table 5
Recombinant protein titer in media alteration experiments.

Media conditions	Control (mg/L)	ELP (mg/L)	A5 4mer (mg/L)	A5 16mer (mg/L)
M9 + 4 g/L Glucose	N/A	28.1 ± 5.9	37.4 ± 3.1	6.0 ± 1.3
LB	N/A	239 ± 23	201 ± 6	53 ± 4
M9 + 4 g/L Gluconate	N/A	20.2 ± 2	43 ± 3.6	4.1 ± 0.8
LB + 20 g/L Gluconate	N/A	41.0 ± 3.7	61.3 ± 4.1	10.0 ± 1.4
LB + 20 g/L Glucose	N/A	31.0 ± 2.7	61.0 ± 3.2	12.0 ± 3.2
M9 + 4 g/L Glucose + 7 amino acids	N/A	60 ± 3.9	73.6 ± 4.7	15.2 ± 1.4
M9 + 20 g/L Glucose + 7 amino acids	N/A	78.0 ± 4.0	60.8 ± 3.7	12.8 ± 1.5
M9 + 4 g/L Glucose + 8 amino acids	N/A	89.6 ± 7.0	87.6 ± 0.8	13.6 ± 0.6
M9 + 4 g/L Glucose + 7 amino acids +10 mM Acetate	N/A	64.0 ± 5.0	42.4 ± 4.4	2.5 ± 0.5
M9 + 4 g/L Glucose + 7 amino acids +30 mM Acetate	N/A	84.1 ± 4.2	37.6 ± 1.6	1.7 ± 0.1
M9 + 4 g/L Glucose + 7 amino acids +90 mM Acetate	N/A	58.8 ± 5.2	13.2 ± 0.1	1.4 ± 0.2

Note: The 7 amino acids are 0.3 g/L of each histidine, isoleucine, phenylalanine, proline, tyrosine, lysine, and methionine. The 8 amino acids are 7 amino acids plus 0.3 g/L glutamate. n = 3, ±standard deviation.

are TCA cycle amino acids), acetate overflow will hurt their production more than other constructs such as ELP. The ELP, A5 4mer, and A5 16mer expressions were carried out in M9 minimal media with 4 g/L glucose (along with 0.3 g/L of each: histidine, isoleucine, phenylalanine, proline, tyrosine, lysine, and methionine) with the addition of 10, 30, or 90 mM sodium acetate at the time of induction. As Table 5 shows, at just 10 mM acetate, there was a severe decrease in the titers of the A5 4mer and A5 16mer constructs. Titers of the A5 16mer were barely detectable at any concentration of exogenous acetate, yielding levels below 3 mg/L. The effect of acetate decreasing silk titer was monotonic for the A5 4mer, with 90 mM acetate yielding a decrease in titer from 73 to 12 mg/L. In contrast, the addition of acetate did not negatively affect the production of the ELP. Titers at 10 and 90 mM acetate are nearly identical to those achieved in the same media without acetate. Interestingly, the ELP titer under 30 mM acetate exceeded that of the baseline media by approximately 24 mg/L (Table 5, Fig. 6).

The starkly different responses of silk and ELP production to acetate show that product toxicity is much more of a bottleneck for silk production than for ELP production. Past work demonstrated that production of the A5 4 and 16mer silk proteins in *E. coli* leads to toxicity, while the ELP appears non-toxic, as shown by severely reduced growth during the expression of a silk construct (Connor et al., 2023). Despite this, the SoluBL21-pLysS strain can achieve 4–33 times higher silk protein titers than other strains, such as BL21. This may be due to unique genetic mutations in strain SoluBL21-pLysS, potentially upregulating several stress responses, including acid stress (Connor et al., 2023). In this context, the strain has higher titers of these toxic silk constructs but remains more vulnerable to the addition of acetate when compared to ELP production. It appears that the addition of any exogenous acetate overwhelms the capabilities of this strain during silk production, with ELP production relatively unaffected.

3.8. Glucose catabolism leads to an undesirable positive feedback loop

Based on strain phenotypes, metabolic flux distributions, and acetate toxicity responses, we suggest a theory that explains our strains' performance in this study. Thermodynamics constrains cells' metabolome, and the absolute metabolite concentrations are highly conserved across all cell types (Park et al., 2016). Microorganisms can inherently resist metabolic flux redistribution brought by artificial metabolic engineering, hence metabolic rigidity (He et al., 2014; Stephanopoulos and Sinskey, 1993; Stephanopoulos and Vallino, 1991). In our previous strain engineering experiences, significant flux redistribution was rare, and flux changes caused by genetic manipulations were usually limited to a few reactions (Abernathy et al., 2019; He et al., 2014, 2017). With high ATP demand for silk production, the cells tend to increase acetate overflow (Holm et al., 2010; Koebmann et al., 2002), but EMP and PP pathway fluxes were rigidly maintained. As discussed before, acetate overflow inhibits the TCA cycle, causes lower ATP production via oxidative phosphorylation, and makes the cells rely more on ATP production via glycolytic substrate-level phosphorylation, forming a vicious positive feedback loop that brings toxicity and metabolic burden to the cells (Fig. 7). The result of this vicious cycle is a lower silk production titer. Cells can decouple this positive feedback (reduce "gain") by co-utilizing high-energy substrates other than glucose (i.e., amino acids), loosening the thermodynamics constraints, and resolving metabolic imbalances (Mannan et al., 2017). In previous studies, the use of glycerol as an alternative carbon source can balance cell metabolism, avoid acetate overflow, and improve recombinant protein production (da Silva et al., 2013). Following this method, 125 mg/L production of a small spidroin in shake flask (Andersson et al., 2017) was scaled up to a high titer of over 20 g/L in a fed-batch bioreactor (Schmuck et al., 2021). Similarly, in this study, growth media with amino acid supplements had much higher production titers, and rich LB media had the best titer across all three engineered strains (Table 5, Fig. 6).

While acetate overflow is specific to *E. coli* that produces

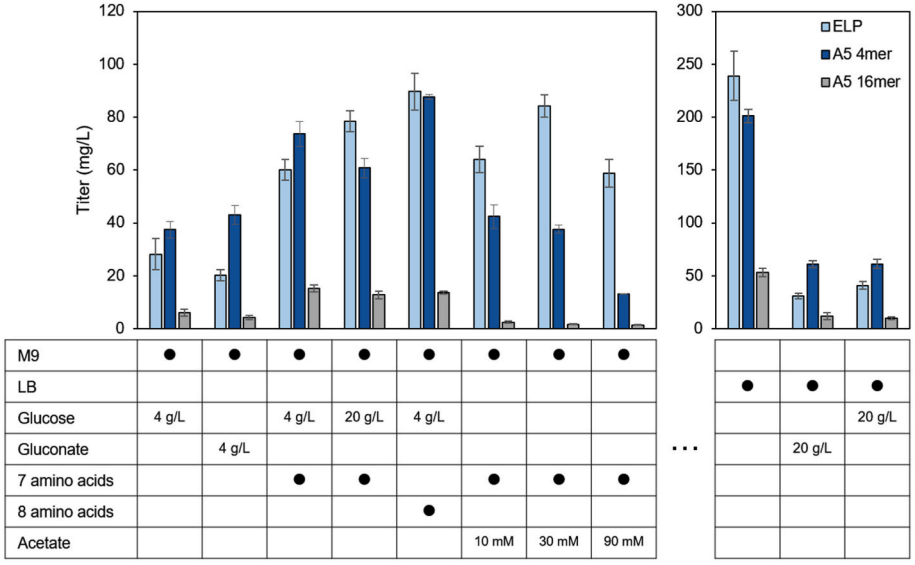

Fig. 6. Recombinant protein titer in media alteration experiments: graphical illustration.
Note: The 7 amino acids are 0.3 g/L of each histidine, isoleucine, phenylalanine, proline, tyrosine, lysine, and methionine. The 8 amino acids are 7 amino acids plus 0.3 g/L glutamate. n = 3, ±standard deviation. Note the Y-axis scale difference between the left and right panels.

Table 6
OD_{600} in media alteration experiments.

Media conditions	Control	ELP	A5 4mer	A5 16mer
M9 + 4 g/L Glucose	1.98 ± 0.05	2.02 ± 0.07	1.13 ± 0.04	1.12 ± 0.03
LB	3.01 ± 0.09	2.73 ± 0.14	2.16 ± 0.06	1.69 ± 0.03
M9 + 4 g/L Gluconate	1.38 ± 0.02	1.38 ± 0.08	1.24 ± 0.05	1.03 ± 0.05
LB + 20 g/L Gluconate	2.60 ± 0.07	1.79 ± 0.07	1.24 ± 0.05	1.08 ± 0.03
LB + 20 g/L Glucose	2.81 ± 0.01	1.92 ± 0.14	1.57 ± 0.04	1.18 ± 0.05
M9 + 4 g/L Glucose +7 amino acids	1.96 ± 0.03	2.03 ± 0.11	1.60 ± 0.02	1.30 ± 0.06
M9 + 20 g/L Glucose +7 amino acids	1.91 ± 0.01	1.95 ± 0.11	1.43 ± 0.03	1.28 ± 0.07
M9 + 4 g/L Glucose +8 amino acids	1.94 ± 0.04	1.93 ± 0.04	1.53 ± 0.01	1.28 ± 0.01
M9 + 4 g/L Glucose +7 amino acids +10 mM Acetate	1.67 ± 0.03	1.50 ± 0.02	1.10 ± 0.07	1.19 ± 0.04
M9 + 4 g/L Glucose +7 amino acids +30 mM Acetate	1.49 ± 0.01	1.54 ± 0.06	1.10 ± 0.08	1.03 ± 0.07
M9 + 4 g/L Glucose +7 amino acids +90 mM Acetate	1.23 ± 0.03	1.21 ± 0.04	0.94 ± 0.04	0.92 ± 0.04

Note: The 7 amino acids are 0.3 g/L of each histidine, isoleucine, phenylalanine, proline, tyrosine, lysine, and methionine. The 8 amino acids are 7 amino acids plus 0.3 g/L glutamate. n = 3, ±standard deviation.

recombinant protein, the positive feedback and metabolic imbalance described in Fig. 7 are common in other constructs. Flux balance analysis showed that due to metabolic burden, the margin between bacterial fitness and efficient recombinant production is very small, hence the "metabolic cliff" (Wu et al., 2016). Microbes have interconnected enzymatic machinery that constrains cellular resources for biosynthesis (Taniguchi et al., 2010). During strain engineering, cell metabolism has to be re-programmed to accommodate the burdens from heterologous enzyme synthesis and bio-productions (Heyland et al., 2011). The metabolic burdens also interact with metabolite inhibitions and induce further stresses on the cell flux network. Metabolic burden limits synthetic biology biomanufacturing because engineered microbial hosts often show impaired fitness and unpredictable metabolic responses in suboptimal bioreactor conditions. Currently, bio-based chemicals from laboratories are difficult to make through the *Valley of Death* to market implementation (Kampers et al., 2022). We need new principles for guiding strain development. In addition to manipulating growth condition and substrate, when control theory meets synthetic biology (Del Vecchio et al., 2016; Hsiao et al., 2018), advances in synthetic biology have suggested other ways to decouple this positive feedback loop and improve strain performance. For example, when producing silk protein in *C. glutamicum*, secreting the silk protein into media (Jin et al., 2022) can avoid the "disturbance" of toxic product accumulation (Fig. 7). Similar to frequency response in the control theory, periodic oscillation of pathway expression can relax metabolic burden and improve productivity (Sowa et al., 2014). Synthetic genetic circuits can add feedforward control to the system and dynamically regulate the metabolic burden brought by the engineered pathway, balancing cell growth and product synthesis (Barajas et al., 2022). However, the current understanding of this dynamic response to heterogeneous production pathway is only qualitative. In future works, molecular acturators can regulate and fine-tune heterologous production pathways. Also, a mathematical model that quantitatively describes control theory elements in Fig. 7 can facilitate better strain design and engineering.

4. Conclusions

This work illustrates a workflow for characterizing and optimizing the recombinant silk fibroin protein production in a novel *E. coli* soluBL21-pLysS strain. We used ^{13}C substrate to identify essential amino acids in media optimization, doubling the production titer of both ELP and silk constructs with 7 amino acids supplementation. The ^{13}C MFA resolved central metabolism flux, and we observed measurable redistributions in ED and TCA fluxes. The genome-scale model showed that cofactors are in shortage during the protein expression, and glutamate production consumed significantly more cellular NADPH than the control strain. Media supplementation of glutamate in the ELP strain relieved NADPH shortage and achieved the same absolute titer increase as 7 amino acids combined. In silk-producing strains, qRT-PCR results confirmed the unusual activation of the ED pathway during silk protein production, but feeding gluconic acid did not significantly increase the protein titer due to low ATP yield in this pathway. We found that sugar/sugar acid metabolism is detrimental to recombinant protein production in *E. coli* soluBL21-pLysS because of the toxic acetic acid overflow, which induces the acid stress response in the cell, reduces TCA cycle flux, and forms an undesired positive feedback loop for acetate overflow. Since the silk protein is rich in TCA cycle amino acids glutamine and

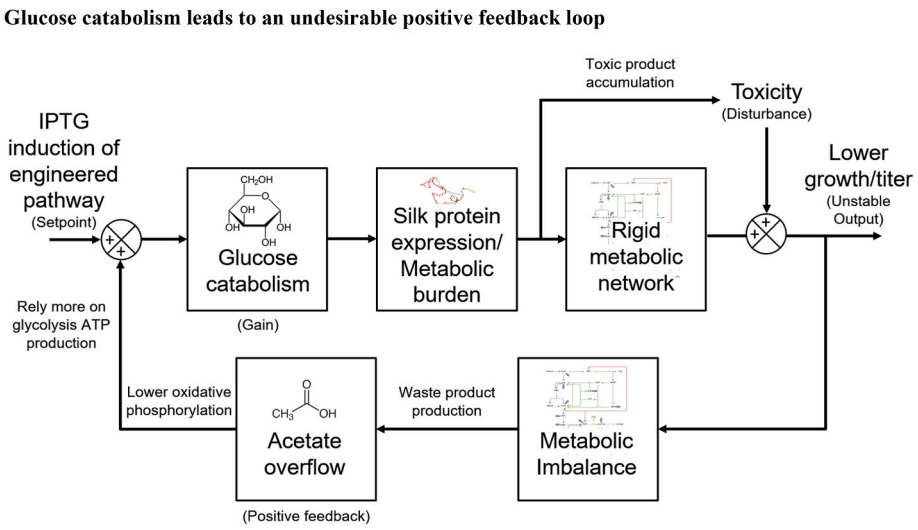

Fig. 7. Using a process control analogy, glucose catabolism in *E. coli* has a positive feedback loop and causes the bottleneck in recombinant silk protein production titer.

proline, acetic overflow is particularly problematic for silk constructs compared to other structural proteins like ELP. Finally, product toxicity to the host cell cannot be explained at the metabolic pathway level and will require additional engineering to overcome. Our findings can help guide future strain engineering of similar highly disordered protein constructs, identify pathways related to high titers, and optimize growth media in a case-by-case scenario.

Author statement

Zhengyang Xiao and Alexander Connor: Conceptualization, Methodology, Validation, Formal Analysis, Investigation, Visualization, Writing – Original draft preparation, revision and editing. Alyssa Worland: carried out experimental work. Yinjie Tang, R. Helen Zha, Mattheos Koffas: Conceptualization, Resources, Funding Acquisition, Supervision, Writing – revision and editing.

Data availability

Data will be made available on request.

Acknowledgments

H.Z. and M.K. would like to acknowledge funding provided from United States NSF award number MCB-2036768.

Appendix A. Supplementary data

Supplementary data to this article can be found online at https://doi.org/10.1016/j.ymben.2023.03.011.

References

Abernathy, M.H., Czajka, J.J., Allen, D.K., Hill, N.C., Cameron, J.C., Tang, Y.J., 2019. Cyanobacterial carboxysome mutant analysis reveals the influence of enzyme compartmentalization on cellular metabolism and metabolic network rigidity. Metab. Eng. 54, 222–231.

Altman, G.H., Diaz, F., Jakuba, C., Calabro, T., Horan, R.L., Chen, J., Lu, H., Richmond, J., Kaplan, D.L., 2003. Silk-based biomaterials. Biomaterials 24, 401–416.

Andersson, M., Jia, Q., Abella, A., Lee, X.-Y., Landreh, M., Purhonen, P., Hebert, H., Tenje, M., Robinson, C.V., Meng, Q., Plaza, G.R., Johansson, J., Rising, A., 2017. Biomimetic spinning of artificial spider silk from a chimeric minispidroin. Nat. Chem. Biol. 13, 262–264.

Au - You, L., Au - Page, L., Au - Feng, X., Au - Berla, B., Au - Pakrasi, H.B., Au - Tang, Y.J., 2012. Metabolic pathway confirmation and discovery through 13C-labeling of proteinogenic amino acids. JoVE e3583.

Barajas, C., Huang, H.-H., Gibson, J., Sandoval, L., Del Vecchio, D., 2022. Feedforward growth rate control mitigates gene activation burden. Nat. Commun. 13, 7054.

Bowen, C.H., Dai, B., Sargent, C.J., Bai, W., Ladiwala, P., Feng, H., Huang, W., Kaplan, D. L., Galazka, J.M., Zhang, F., 2018. Recombinant spidroins fully replicate primary mechanical properties of natural spider silk. Biomacromolecules 19, 3853–3860.

Cardoso, V.M., Campani, G., Santos, M.P., Silva, G.G., Pires, M.C., Gonçalves, V.M., Giordano, R.d.C., Sargo, C.R., Horta, A.C., Zangirolami, T.C., 2020. Cost analysis based on bioreactor cultivation conditions: production of a soluble recombinant protein using Escherichia coli BL21 (DE3). Biotechnology Reports 26, e00441.

Collins, T., Azevedo-Silva, J., da Costa, A., Branca, F., Machado, R., Casal, M., 2013. Batch production of a silk-elastin-like protein in E. coli BL21(DE3): key parameters for optimisation. Microb. Cell Factories 12, 21.

Connor, A., Wigham, C., Bai, Y., Rai, M., Nassif, S., Koffas, M., Zha, R.H., 2023. Novel insights into construct toxicity, strain optimization, and primary sequence design for producing recombinant silk fibroin and elastin-like peptide in E. coli. Metabolic Engineering Communications, e00219.

Czajka, J.J., Kambhampati, S., Tang, Y.J., Wang, Y., Allen, D.K., 2020. Application of stable isotope tracing to elucidate metabolic dynamics during yarrowia lipolytica α-ionone fermentation. iScience 23, 100854.

da Silva, A.J., Horta, A.C.L., Velez, A.M., Iemma, M.R.C., Sargo, C.R., Giordano, R.L.C., Novo, M.T.M., Giordano, R.C., Zangirolami, T.C., 2013. Non-conventional induction strategies for production of subunit swine erysipelas vaccine antigen in rE. coli fed-batch cultures. SpringerPlus 2, 322.

Del Vecchio, D., Dy, A.J., Qian, Y., 2016. Control theory meets synthetic biology. J. R. Soc. Interface 13, 20160380.

Ebrahim, A., Lerman, J.A., Palsson, B.O., Hyduke, D.R., 2013. COBRApy: COnstraints-based reconstruction and analysis for Python. BMC Syst. Biol. 7, 74.

Eiteman, M.A., Altman, E., 2006. Overcoming acetate in Escherichia coli recombinant protein fermentations. Trends Biotechnol. 24, 530–536.

Fischer, E., Sauer, U., 2005. Large-scale in vivo flux analysis shows rigidity and suboptimal performance of Bacillus subtilis metabolism. Nat. Genet. 37, 636–640.

Flamholz, A., Noor, E., Bar-Even, A., Liebermeister, W., Milo, R., 2013. Glycolytic strategy as a tradeoff between energy yield and protein cost. Proc. Natl. Acad. Sci. USA 110, 10039–10044.

Gatesy, J., Hayashi, C., Motriuk, D., Woods, J., Lewis, R., 2001. Extreme diversity, conservation, and convergence of spider silk fibroin sequences. Science 291, 2603–2605.

Glick, B.R., 1995. Metabolic load and heterologous gene expression. Biotechnol. Adv. 13, 247–261.

Gosline, J.M., Guerette, P., Ortlepp, C., Savage, K., 1999. The mechanical design of spider silks: from fibroin sequence to mechanical function. J. Exp. Biol. 202, 3295–3303.

Hädicke, O., Klamt, S., 2017. EColiCore2: a reference network model of the central metabolism of Escherichia coli and relationships to its genome-scale parent model. Sci. Rep. 7, 39647.

Hardy, J.G., Römer, L.M., Scheibel, T.R., 2008. Polymeric materials based on silk proteins. Polymer 49, 4309–4327.

He, L., Wu, S.G., Zhang, M., Chen, Y., Tang, Y.J., 2016. WUFlux: an open-source platform for 13C metabolic flux analysis of bacterial metabolism. BMC Bioinf. 17, 444.

He, L., Xiao, Y., Gebreselassie, N., Zhang, F., Antoniewicz, M.R., Tang, Y.J., Peng, L., 2014. Central metabolic responses to the overproduction of fatty acids in Escherichia coli based on 13C-metabolic flux analysis. Biotechnol. Bioeng. 111, 575–585.

He, L., Xiu, Y., Jones, J.A., Baidoo, E.E., Keasling, J.D., Tang, Y.J., Koffas, M.A., 2017. Deciphering flux adjustments of engineered E. coli cells during fermentation with changing growth conditions. Metab. Eng. 39, 247–256.
Heyland, J., Blank, L.M., Schmid, A., 2011. Quantification of metabolic limitations during recombinant protein production in Escherichia coli. J. Biotechnol. 155, 178–184.
Hoffmann, F., Rinas, U., 2004. Stress induced by recombinant protein production in Escherichia coli. Physiological stress responses in bioprocesses 73–92.
Holland, C., Numata, K., Rnjak-Kovacina, J., Seib, F.P., 2019. The biomedical use of silk: past, present, future. Advanced healthcare materials 8, 1800465.
Hollinshead, W., He, L., Tang, Y.J., 2019. 13C-Fingerprinting and metabolic flux analysis of bacterial metabolisms. In: Santos, C.N.S., Ajikumar, P.K. (Eds.), Microbial Metabolic Engineering: Methods and Protocols. Springer New York, New York, NY, pp. 215–230.
Hollinshead, W.D., Rodriguez, S., Martin, H.G., Wang, G., Baidoo, E.E.K., Sale, K.L., Keasling, J.D., Mukhopadhyay, A., Tang, Y.J., 2016. Examining Escherichia coli glycolytic pathways, catabolite repression, and metabolite channeling using Δpfk mutants. Biotechnol. Biofuels 9, 212.
Holm, A.K., Blank, L.M., Oldiges, M., Schmid, A., Solem, C., Jensen, P.R., Vemuri, G.N., 2010. Metabolic and transcriptional response to cofactor perturbations in Escherichia coli. J. Biol. Chem. 285, 17498–17506.
Hsiao, V., Swaminathan, A., Murray, R.M., 2018. Control theory for synthetic biology: recent advances in system characterization, control design, and controller implementation for synthetic biology. IEEE Control Syst. Mag. 38, 32–62.
Jansson, R., Lau, C.H., Ishida, T., Ramström, M., Sandgren, M., Hedhammar, M., 2016. Functionalized silk assembled from a recombinant spider silk fusion protein (Z-4RepCT) produced in the methylotrophic yeast Pichia pastoris. Biotechnol. J. 11, 687–699.
Jensen, E.B., Carlsen, S., 1990. Production of recombinant human growth hormone in Escherichia coli: expression of different precursors and physiological effects of glucose, acetate, and salts. Biotechnol. Bioeng. 36, 1–11.
Jin, Q., Pan, F., Hu, C.-F., Lee, S.Y., Xia, X.-X., Qian, Z.-G., 2022. Secretory production of spider silk proteins in metabolically engineered Corynebacterium glutamicum for spinning into tough fibers. Metab. Eng. 70, 102–114.
Kaleta, C., Schäuble, S., Rinas, U., Schuster, S., 2013. Metabolic costs of amino acid and protein production in Escherichia coli. Biotechnol. J. 8, 1105–1114.
Kampers, L.F., Asin-Garcia, E., Schaap, P.J., Wagemakers, A., dos Santos, V.A.M., 2022. Navigating the Valley of death: perceptions of industry and academia on production platforms and opportunities in biotechnology. EFB Bioeconomy Journal 2, 100033.
Kayser, A., Weber, J., Hecht, V., Rinas, U., 2005. Metabolic flux analysis of Escherichia coli in glucose-limited continuous culture. I. Growth-rate-dependent metabolic efficiency at steady state. Microbiology 151, 693–706.
Koebmann, B.J., Westerhoff, H.V., Snoep, J.L., Nilsson, D., Jensen, P.R., 2002. The glycolytic flux in Escherichia coli is controlled by the demand for ATP. J. Bacteriol. 184, 3909–3916.
Kumar, J., Chauhan, A.S., Shah, R.L., Gupta, J.A., Rathore, A.S., 2020. Amino acid supplementation for enhancing recombinant protein production in E. coli. Biotechnol. Bioeng. 117, 2420–2433.
Lazaris, A., Arcidiacono, S., Huang, Y., Zhou, J.F., Duguay, F., Chretien, N., Welsh, E.A., Soares, J.W., Karatzas, C.N., 2002. Spider silk fibers spun from soluble recombinant silk produced in mammalian cells. Science 295, 472–476.
Luli, G.W., Strohl, W.R., 1990. Comparison of growth, acetate production, and acetate inhibition of Escherichia coli strains in batch and fed-batch fermentations. Appl. Environ. Microbiol. 56, 1004–1011.
Mannan, A.A., Liu, D., Zhang, F., Oyarzún, D.A., 2017. Fundamental design principles for transcription-factor-based metabolite biosensors. ACS Synth. Biol. 6, 1851–1859.
Marelli, B., Brenckle, M., Kaplan, D.L., Omenetto, F.G., 2016. Silk fibroin as edible coating for perishable food preservation. Sci. Rep. 6, 1–11.
Millard, P., Enjalbert, B., Uttenweiler-Joseph, S., Portais, J.-C., Létisse, F., 2021. Control and regulation of acetate overflow in Escherichia coli. Elife 10, e63661.
Motta, A., Fambri, L., Migliaresi, C., 2002. Regenerated silk fibroin films: thermal and dynamic mechanical analysis. Macromol. Chem. Phys. 203, 1658–1665.
O'Brien, E.J., Monk, J.M., Palsson, B.O., 2015. Using genome-scale models to predict biological capabilities. Cell 161, 971–987.
Özkan, P., Sariyar, B., Ütkür, F.Ö., Akman, U., Hortaçsu, A., 2005. Metabolic flux analysis of recombinant protein overproduction in Escherichia coli. Biochem. Eng. J. 22, 167–195.
Park, J.O., Rubin, S.A., Xu, Y.-F., Amador-Noguez, D., Fan, J., Shlomi, T., Rabinowitz, J. D., 2016. Metabolite concentrations, fluxes and free energies imply efficient enzyme usage. Nat. Chem. Biol. 12, 482–489.
Rugbjerg, P., Sommer, M.O.A., 2019. Overcoming genetic heterogeneity in industrial fermentations. Nat. Biotechnol. 37, 869–876.
Rui, B., Shen, T., Zhou, H., Liu, J., Chen, J., Pan, X., Liu, H., Wu, J., Zheng, H., Shi, Y., 2010. A systematic investigation of Escherichia coli central carbon metabolism in response to superoxide stress. BMC Syst. Biol. 4, 1–12.
San Román, M., Cancela, H., Acerenza, L., 2014. Source and regulation of flux variability in Escherichia coli. BMC Syst. Biol. 8, 1–11.
Sarkar, A., Connor, A.J., Koffas, M., Zha, R.H., 2019. Chemical synthesis of silk-mimetic polymers. Materials 12, 4086.
Scheller, J., Henggeler, D., Viviani, A., Conrad, U., 2004. Purification of spider silk-elastin from transgenic plants and application for human chondrocyte proliferation. Transgenic Res. 13, 51–57.
Schmuck, B., Greco, G., Barth, A., Pugno, N.M., Johansson, J., Rising, A., 2021. High-yield production of a super-soluble miniature spidroin for biomimetic high-performance materials. Mater. Today 50, 16–23.
Shuler, M.L., Kargi, F., 2002. Bioprocess Engineering: Basic Concepts. Prentice Hall.
Sowa, S.W., Baldea, M., Contreras, L.M., 2014. Optimizing metabolite production using periodic oscillations. PLoS Comput. Biol. 10, e1003658.
Stephanopoulos, G., Sinskey, A.J., 1993. Metabolic engineering—methodologies and future prospects. Trends Biotechnol. 11, 392–396.
Stephanopoulos, G., Vallino, J.J., 1991. Network rigidity and metabolic engineering in metabolite overproduction. Science 252, 1675–1681.
Suarez, D., Kilikian, B.J.P., 2000. Acetic acid accumulation in aerobic growth of recombinant Escherichia coli. Process Biochemistry 35, 1051–1055.
Taniguchi, Y., Choi, P.J., Li, G.-W., Chen, H., Babu, M., Hearn, J., Emili, A., Xie, X.S., 2010. Quantifying E. coli proteome and transcriptome with single-molecule sensitivity in single cells. Science 329, 533–538.
Teulé, F., Cooper, A.R., Furin, W.A., Bittencourt, D., Rech, E.L., Brooks, A., Lewis, R.V., 2009. A protocol for the production of recombinant spider silk-like proteins for artificial fiber spinning. Nat. Protoc. 4, 341–355.
Tokareva, O., Jacobsen, M., Buehler, M., Wong, J., Kaplan, D.L., 2014. Structure–function–property–design interplay in biopolymers: spider silk. Acta Biomater. 10, 1612–1626.
Tokareva, O., Michalczechen-Lacerda, V.A., Rech, E.L., Kaplan, D.L., 2013. Recombinant DNA production of spider silk proteins. Microb. Biotechnol. 6, 651–663.
Tsioris, K., Tilburey, G.E., Murphy, A.R., Domachuk, P., Kaplan, D.L., Omenetto, F.G., 2010. Functionalized-silk-based active optofluidic devices. Adv. Funct. Mater. 20, 1083–1089.
Vepari, C., Kaplan, D.L., 2007. Silk as a biomaterial. Prog. Polym. Sci. 32, 991–1007.
Weber, J., Hoffmann, F., Rinas, U., 2002. Metabolic adaptation of Escherichia coli during temperature-induced recombinant protein production: 2. Redirection of metabolic fluxes. Biotechnol. Bioeng. 80, 320–330.
Wen, H., Lan, X., Zhang, Y., Zhao, T., Wang, Y., Kajiura, Z., Nakagaki, M., 2010. Transgenic silkworms (Bombyx mori) produce recombinant spider dragline silk in cocoons. Mol. Biol. Rep. 37, 1815–1821.
Whittall, D.R., Baker, K.V., Breitling, R., Takano, E., 2021. Host systems for the production of recombinant spider silk. Trends Biotechnol. 39, 560–573.
Wu, G., Yan, Q., Jones, J.A., Tang, Y.J., Fong, S.S., Koffas, M.A.G., 2016. Metabolic burden: cornerstones in synthetic biology and metabolic engineering applications. Trends Biotechnol. 34, 652–664.
Yang, Y.-T., Aristidou, A.A., San, K.-Y., Bennett, G.N., 1999. Metabolic flux analysis ofEscherichia coliDeficient in the acetate production pathway and expressing theBacillus subtilisAcetolactate synthase. Metab. Eng. 1, 26–34.
Yang, Y.-X., Qian, Z.-G., Zhong, J.-J., Xia, X.-X., 2016. Hyper-production of large proteins of spider dragline silk MaSp2 by Escherichia coli via synthetic biology approach. Process Biochemistry 51, 484–490.
You, L., Liu, H., Blankenship, R.E., Tang, Y.J., 2015. Using photosystem I as a reporter protein for 13C analysis in a coculture containing cyanobacterium and a heterotrophic bacterium. Anal. Biochem. 477, 86–88.
You, L., Page, L., Feng, X., Berla, B., Pakrasi, H.B., Tang, Y.J., 2012. Metabolic pathway confirmation and discovery through (13)C-labeling of proteinogenic amino acids. J. Vis. Exp. e3583.
Young, J.D., 2014. 13C metabolic flux analysis of recombinant expression hosts. Curr. Opin. Biotechnol. 30, 238–245.
Zhuang, W.Q., Yi, S., Feng, X., Zinder, S.H., Tang, Y.J., Alvarez-Cohen, L., 2011. Selective utilization of exogenous amino acids by Dehalococcoides ethenogenes strain 195 and its effects on growth and dechlorination activity. Appl. Environ. Microbiol. 77, 7797–7803.